CrossMark

# Lagrangian-based Hydrodynamic Model for Traffic Data Fusion on Freeways

Ke Han[1] · Tao Yao[2] · Chaozhe Jiang[3] ·
Terry L. Friesz[2]

**Abstract** This paper conducts a comprehensive study of the Lagrangian-based hydrodynamic model with application to highway state estimation. Our analysis is motivated by the practical problems of freeway traffic monitoring and estimation using multi-source data measured from mobile devices and fixed sensors. We conduct rigorous mathematical analysis on the Hamilton-Jacobi representation of the Lighthill-Whitham-Richards model in the transformed coordinates, and derive explicit and closed-form solutions with piecewise affine initial, boundary, and internal conditions, based on the variational principle. A numerical study of the Mobile Century field experiment demonstrates some unique features and the effectiveness in traffic estimation of the Lagrangian-based model.

✉ Chaozhe Jiang
  jiangchaozhe@163.com

  Ke Han
  k.han@imperial.ac.uk

  Tao Yao
  tyy1@engr.psu.edu

  Terry L. Friesz
  tfriesz@psu.edu

1   Department of Civil and Environmental Engineering, Imperial College London,
    London SW7 2BU, UK

2   Department of Industrial and Manufacturing Engineering, Pennsylvania State University,
    State College, PA 16802, USA

3   College of Traffic and Transportation, Southwest Jiaotong University, Chengdu, China

## 1 Introduction

Highway traffic state estimation is one of the essential components in traffic management. From an estimation perspective, it is desirable to have a substantial amount of information available. Technologies of traffic monitoring such as Eulerian sensing (loop detector, video camera) and Lagrangian sensing (on-board smart phone or GPS) provide large and dense data sets and potentially lead to more accurate estimation. However, from a modeling point of view, the inclusion of additional data usually leads to inconsistency with an established traffic model, such as the Lighthill-Whitham-Richards (LWR) model (Lighthill and Whitham 1955; Richards 1956). Such incompatibility between observations (value conditions) and the mathematical model is often manifested in the non-existence of entropy solution to the *partial differential equation* (PDE).

The well-known hydrodynamic traffic models (Lighthill and Whitham 1955; Richards 1956) have been mostly formulated in Eulerian coordinates (time $t$, location $x$); see Bressan and Han (2011, 2012); Claudel and Bayen (2010a, b); Daganzo (2005, 2006); Lighthill and Whitham (1955); Newell (1993) and Richards (1956). The Eulerian-based model describes vehicle density and flux using a scalar conservation law. This type of PDE is usually associated with initial/boundary value conditions which are inherently Eulerian. Initial and boundary value problems, if well posed, leads to the existence and uniqueness of a solution (Bressan 2000; Evans 2010; Garavello et al. 2016).

While a spectrum of mathematical analyses and computational methods exist in the current literature that deal with initial/boundary value problems for partial differential equations (Daganzo 2005, 2006; Evans 2010; Le Floch 1988; LeVeque 1902), these are insufficient to address the problems of traffic state estimation and reconstruction arising in the context of mobile sensing. Indeed, the fast developing and maturing traffic monitoring systems, with Lagrangian sensing capabilities through on-board devices, enables higher coverage of the physical domain and requires fast and accurate data fusing techniques. Claudel and Bayen (2010a, b, 2011) took the first step in integrating fixed and mobile sensing into a single Hamilton-Jacobi equation in Eulerian coordinates. This was done through the notion of *internal boundary conditions* (IBC), which are internal to the spatio-temporal domain of the PDE. In order to avoid the issue of non-existence of solutions, Claudel and Bayen (2010a, b) adapted a more general solution class known as the Barron-Jensen/Frankowska (BJ/F) solutions (Aubin 2009; Barron and Jensen 1990). This type of solution, in contrast to the viscosity solution, is lower-semicontinuous, and the corresponding computational method is known as the generalized Lax-Hopf formula.

The *Lagrangian coordinates system* (LCS), applied to hydrodynamic modeling, was introduced in Courant and Friedrichs (1999) in the context of gas dynamics and subsequently studied in, e.g. Leclercq et al. (2007) and Laval and Leclercq (2013). It consists of two independent parameters: time ($t$) and vehicle label ($n$). In contrast to

the Eulerian coordinate system, the LCS is trajectory-based, i.e. it describes the evolution of variables of interest along a particle trajectory. The hydrodynamic traffic models in Lagrangian coordinates describes vehicle spacing and vehicle speed using a scalar conservation law. A detailed review of this model will be presented later in this article. The idea conveyed in the Lagrangian-based approach, i.e. the trajectory-based description of traffic flow, provides new insights of the hydrodynamic model. The LCS establishes a natural modeling framework for moving vehicles regardless of their physical locations, which can be potentially applied to vehicle-based cyber-physical systems such as mobile networking or mobile internet. With increasing availability of floating car data, as well as car-to-car communication, a vehicle-based traffic model could offer additional capabilities and insights unavailable in a location-based model. The Lagrangian coordinate system and its applications to traffic flow theory, network modeling and intelligent transportation system remain a promising yet less exploited field.

Recent studies (Leclercq et al. 2007; Yuan et al. 2011) showed the computational advantage of Lagrangian-based PDE over Eulerian-based PDE in terms of finite difference algorithms. The Lagrangian-based conservation law allows only non-negative wave propagation speed instead of both positive and negative wave speeds as in the Eulerian-based model, which reduces the Godunov scheme (Godunov 1959) to a simple upwind scheme. As we will see later in this article, the Lagrangian-based model also admits a simpler solution representation when the Lax-Hopf formula is used as the computational method. Despite these desirable features, the Lagrangian-based traffic models are not sufficiently studied and understood in the current literature, especially its potential contributions to real-world traffic estimation, data assimilation, inverse modeling as well as mobile networking, which has motivated our work presented in this paper.

This article conducts a comprehensive study of the Lagrangian-based traffic model in terms of model derivation and justification, value conditions, numerical algorithm as well as its application to traffic state estimation/reconstruction. In particular, we adapt the notion of viability episolution (Claudel and Bayen 2010a, b) to the Hamilton-Jacobi equation. As previously mentioned, the Lagrangian-based approach yields simpler solution representation than the Eulerian-based approach. Moreover, the resulting solution in Lagrangian coordinates provides easy access to vehicle-based information such as vehicle trajectory and velocity field, which are not directly recovered through Eulerian-based models. Specific technical contents of this article are as follows.

1  We show the relationship between viscosity solutions of the Eulerian and Lagrangian based Hamilton-Jacobi equations. To our knowledge, this is the first rigorous results regarding the equivalence between the H-J equations in these two coordinate systems.
2  We present a framework for fusing both Eulerian (location-fixed) and Lagrangian (vehicle-fixed) sensing data into the Lagrangian PDE. By applying the viability theory and generalized Lax-Hopf formula (Aubin 2009; Claudel and Bayen 2010a, b) to the Lagrangian based Hamilton-Jacobi equation. We provide closed-form solution with piecewise affine value conditions.
3.  Through a numerical study of the *Mobile Century* field experiment (Herrera et al. 2009), we demonstrate the practicality and convenience of using car label as a

free variable in the highway traffic models and the capability of Lagrangian-based PDE to perform data fusing, this is applied to highway traffic estimation and reconstruction.

The rest of the article is organized as follows: in Section 2, we discuss the hydro-dynamic traffic model in the transformed coordinate system. Section 3 introduces the viability episolutions of the Hamilton-Jacobi equation and generalized Lax-Hopf formula. Both Eulerian and Lagrangian sensing data are discussed and integrated into the Lagrangian PDE. Section 4 conducts further investigation of the Lax-Hopf formula in the presence of piecewise affine value conditions and derives explicit solutions to the Lagrangian PDE with various value conditions. Finally, in Section 5 we apply the Lagrangian-based model and methodology to a real-world traffic estimation problem, using data collected from the Mobile Century field experiment (Herrera et al. 2009).

## 2 The LWR Model in Transformed Coordinates

In this section, we present and discuss the LWR model in Eulerian and Lagrangian coordinates. The transformation between these two coordinate systems is made through a function inversion under minor assumptions. Along with the Lagrangian coordinates comes a new equation describing the traffic dynamics, which will be related to the original equation in Eulerian coordinates; the two equations will be respectively presented in Sections 2.1 and 2.2. Result on the equivalence of solutions of both equations is established in Section 2.3.

### 2.1 The LWR Model in Eulerian Coordinates

Traditionally, the LWR model has been formulated in Eulerian coordinates $(t, x)$ as a scalar conservation law (Lighthill and Whitham 1955; Richards 1956):

$$\frac{\partial}{\partial t}\rho(t, x) + \frac{\partial}{\partial x}f(\rho(t, x)) = 0 \qquad (t, x) \in [0, +\infty) \times [0, L] \qquad (2.1)$$

where the model concerns with vehicle density $\rho(t, x)$ and flow (flux) $f(\rho(t, x))$. The fundamental diagram is a concave function of the density $\rho$:

$$f(\rho) = \rho\, v(\rho) \qquad \rho \in [0, \rho_{\max}] \qquad (2.2)$$

where $\rho_{\max}$ is the jam density and the vehicle speed $v(\rho) \in [0, v_{\max}]$ is a decreasing function of density, $v_{\max}$ denotes the free flow speed. The flux function $f(\cdot)$ is assumed to be concave with maximal value $M$ attained at $\rho^*$, $M$ is recognized as the flow capacity, and $\rho^*$ is called the critical density. See Fig. 1 for some examples of the density-flow functional relationship.

We introduce the Moskowitz function $N(\cdot, \cdot)$ (Moskowitz 1965; Claudel and Bayen 2010a, b), defined via the following identities

$$N(t_2, x_2) - N(t_1, x_1) = -\int_{x_1}^{x_2} -\rho(t_1, x)\, dx + \int_{t_1}^{t_2} f\left(\rho(t, x_2)\right) dt \qquad (2.3)$$

In other words, $N(t, x)$ is the cumulative vehicle count at location $x$ by the time $t$. The properties of the Moskowitz function have been extensively studied, for instance in Newell (1993), and we have the identities

$$\frac{\partial}{\partial t} N(t, x) = f\left(\rho(t, x)\right), \qquad \frac{\partial}{\partial x} N(t, x) = -\rho(t, x) \qquad \text{almost everywhere}$$
$$(2.4)$$

It is shown, for example in Evans (2010), that if $\rho(t, x)$ is the weak entropy solution to (2.1), then the corresponding Moskowitz function defined in (2.3) is the viscosity solution to the following Hamilton-Jacobi Eq. (2.5) .

$$\frac{\partial}{\partial t} N(t, x) - f\left(-\frac{\partial}{\partial x} N(t, x)\right) = 0 \qquad (2.5)$$

Note that a viscosity solution to the Eq. (2.5) is Lipschitz continuous, but not necessarily continuous differentiable due to shocks in density $\rho(t, x)$. There exists, however, other classes of solutions to Hamilton-Jacobi Eq. (2.5), for example, the lower-semicontinuous Barron-Jensen/Frankowska solutions derived through viability theory (Aubin 2009; Barron and Jensen 1990; Frankowska 1993). This type of solution only need to satisfy the value conditions in the inequality sense, and can be obtained using the generalized Lax-Hopf formula. We will apply this notion of solutions to the Hamilton-Jacobi equations later in this article.

The model described above is Eulerian-based, i.e. in the coordinates representing space and time. The goal of Section 2.2 is to express the LWR model in the Lagrangian coordinate system $(t, n)$, where $n$ represents vehicle label. The Lagrangian coordinates are concerned with a particular car, and move with it in the space-time domain. Note that in the continuum, $n$ is treated as a real number. In the Lagrangian system, the focus is no longer the density or flow at a point $(t, x)$, but instead the velocity and location of the vehicle identified by $(t, n)$.

## 2.2 The LWR Model in the Lagrangian Coordinates

Now we want to make the coordinate transformation from $(t, x)$ to $(t, n)$, where the quantity $n$ is given by the Moskowitz function

$$n = N(t, x) \qquad (2.6)$$

representing the cumulative vehicles that has passed location $x$ by time $t$. Throughout the rest of this article, we assume the vehicle density is uniformly positive, i.e. there exists $\delta > 0$ such that

$$\rho(t, x) \geq \delta, \qquad \forall (t, x)$$

This assumption does not compromise the validity or applicability of the model, because if a vacuum state occurs in a segment of road, it separates two independent sub problems, where the solution of one does not affect that of the other. Notice that

by this assumption, $n = N(t, \cdot)$ is a strictly decreasing function of $x$, whose inverse will be denoted

$$x = X(t, n) \tag{2.7}$$

where $X(t, n)$ represents the location of vehicle labeled $n$ at time $t$. The transformation of the *Eulerian coordinates* $(t, x)$ and *Lagrangian coordinates* $(t, n)$ is now defined by (2.6) and (2.7). Notice that the vehicle label $n$ is treated as a continuum.

Denote the velocity of vehicle labeled $n$ at time $t$ to be $v(t, n)$, the spacing (reciprocal of density) around vehicle labeled $n$ at time $t$ to be $s(t, n)$. Note that $s(t, n)$ can be interpreted as the space occupied by the vehicle. For $t_1 > t_2$, $n_1 > n_2$, we deduce the following identities:

$$X(t_1, n) - X(t_2, n) = \int_{t_2}^{t_1} v(\tau, n) \, d\tau, \qquad X(t, n_1) - X(t, n_2) = - \int_{n_2}^{n_1} s(t, n) \, dn \tag{2.8}$$

The meanings of (2.8) are straightforward: displacement ($X$) is integral of speed ($v$) over time ($t$); the distance between vehicles $n_1$ and $n_2$ is the integral of car spacings over all cars in between. Notice that car $n_1$ is ahead of car $n_2$. We can rewrite (2.8) as follows

$$\frac{\partial}{\partial t} X(t, n) = v(t, n), \qquad \frac{\partial}{\partial n} X(t, n) = -s(t, n) \qquad \text{almost everywhere} \tag{2.9}$$

where $X(t, n)$, $v(t, n)$ and $s(t, n)$ denote the location, velocity and spacing of vehicle labeled $n$ at time $t$, respectively.

*Remark 2.1* It is well-known that the viscosity solution $N(t, x)$ to (2.5) is Lipschitz continuous. The assumption of uniformly positive density implies that $X(t, n)$ is also Lipschitz continuous, then by Rademacher's theorem it is almost everywhere differentiable, but may have countably many kinks due to discontinuities (shocks). Thus we need to emphasize "almost everywhere" for the validity of (2.4) and (2.9).

Before we introduce the Hamilton-Jacobi equation in Lagrangian coordinates, we need to articulate the spacing-velocity relationship. Given the density-velocity function $\rho \mapsto v(\rho)$, define $\psi : [1/\rho_{\max}, +\infty) \to [0, v_{\max}]$

$$\psi(s) \doteq v(1/s) \tag{2.10}$$

then $\psi(s(t, n))$ equals velocity $v(t, n)$, we thus deduce from (2.9) that

$$\frac{\partial}{\partial t} X(t, n) - \psi \left( -\frac{\partial}{\partial n} X(t, n) \right) = 0 \tag{2.11}$$

The Hamiltonian $\psi(\cdot)$ expresses vehicle velocity as a function of spacing, and we stipulate that it is a continuous, concave function. $\psi(\cdot)$ is uniquely determined by the density-velocity relationship, therefore there is a one-to-one correspondence between $\psi(\cdot)$ and the fundamental diagram $f(\cdot)$. Examples of different fundamental diagrams and their corresponding $\psi(\cdot)$ are shown in Fig. 1.

We also deduce informally from (2.11) the scalar conservation law

$$\frac{\partial}{\partial t} s(t,\, n) + \frac{\partial}{\partial n} \psi\,(s(t,\, n)) = 0 \tag{2.12}$$

by the word 'informally', we imply that before working with (2.12), one needs to establish properties of the weak solution such as existence/uniqueness and related it to the entropy solution of the original conservation law (2.1).

In the rest of this article, we focus on the Hamilton-Jacobi Eq. (2.11) in Lagrangian coordinates, its initial/boundary/internal boundary conditions, numerical solution and applications to highway traffic estimation. Section 2.3 is devoted to justifying Eq. (2.11).

## 2.3 Viscosity Solutions to the Hamilton-Jacobi Equations

The main purpose of this section is to justify the Hamilton-Jacobi equation in Lagrangian coordinates (2.11), in the sense of viscosity solutions. Recent work (Leclercq et al. 2007; Yuan et al. 2011) refers to the equivalence of weak solutions to a system of conservation laws in gas dynamics (Wagner 1987), which, however, does not involve Hamilton-Jacobi equations, and the result does not apply immediately to scalar conservation laws. In order to provide a solid foundation of our work based on Hamilton-Jacobi equation, we provide a mathematical analysis of the H-J solutions in both coordinate systems.

We start with a very general definition of viscosity solution of Hamilton-Jacobi equation in the form

$$u_t + H(\nabla u) = 0 \tag{2.13}$$

where the unknown $u(t,\, x) \in \mathbb{R}^m$ and $\nabla u$ is the gradient of $u$ with respect to $x$. For simplicity of notations, the subscript denotes partial differentiation. In what follows, $C$, $C^1$ denotes the set of continuous and continuously differentiable functions, respectively.
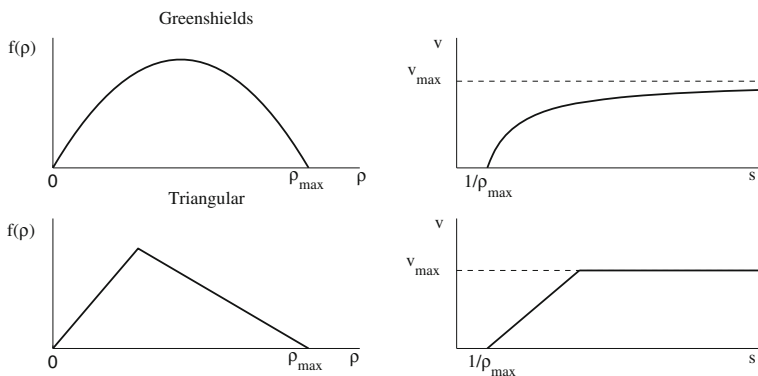


**Fig. 1** Hamiltonians in Eulerian and Lagrangian coordinates. Left: the Greenshields and Triangular fundamental diagram. Right: the equivalent spacing-velocity curve

**Definition 2.2** A function $u \in C(\Omega)$ is a viscosity subsolution of (2.13) if, for every $C^1$ function $\varphi = \varphi(t, x)$ such that $u - \varphi$ has a local maximum at $(t, x)$, there holds

$$\varphi_t(t, x) + H(\nabla\varphi) \leq 0 \qquad (2.14)$$

Similarly, $u \in C(\Omega)$ is a viscosity supersolution of (2.13) if, for every $C^1$ function $\varphi = \varphi(t, x)$ such that $u - \varphi$ has a local minimum at $(t, x)$, there holds

$$\varphi_t(t, x) + H(\nabla\varphi) \geq 0 \qquad (2.15)$$

We say that $u$ is a viscosity solution of (2.13) if it is both a supersolution and a subsolution in the viscosity sense.

*Remark 2.3* If $u$ is a $C^1(\Omega)$ function and satisfies (2.13) at every $x \in \Omega$, then $u$ is also a solution in the viscosity sense. Conversely, if $u$ is a viscosity solution, then the equality must hold at every point $x$ where $u$ is differentiable. In particular, if $u$ is Lipschitz continuous, then it is almost everywhere differentiable, hence (2.13) holds almost everywhere in $\Omega$.

The aim of this section is to establish equivalence analysis of the viscosity solutions of

$$N_t(t, x) - f(-N_x(t, x)) = 0 \qquad (2.16)$$

$$X_t(t, n) - \psi(-X_n(t, n)) = 0 \qquad (2.17)$$

A simple calculation shows that $\psi(s) = s f(1/s)$. The following theorem establishes the connection between (2.16) and (2.17).

**Theorem 2.4** *Assume that $N(t, x)$, $(t, x) \in \Omega \subset (-\infty, +\infty) \times \mathbb{R}^n$, is a viscosity solution to (2.16), furthermore, assume that the density is uniformly positive, i.e. $\rho(t, x) \geq \delta > 0$, $\forall (t, x) \in \Omega$. Then function $X(t, \cdot)$ obtained by inverting $N(t, \cdot)$ is a viscosity solution to (2.17).*

*Proof* By assumption, $N(t, \cdot)$ is strictly decreasing with

$$\delta |x_1 - x_2| \leq |N(t, x_1) - N(t, x_2)| \leq \rho_{max} |x_1 - x_2| \qquad \forall x_1, x_2$$

then $X(t, \cdot)$ is also strictly decreasing with

$$1/\rho_{max}|n_1 - n_2| \leq |X(t, n_1) - X(t, n_2)| \leq 1/\delta |n_1 - n_2| \qquad \forall n_1, n_2 \quad (2.18)$$

We start by showing that $X(\cdot, \cdot)$ is a subsolution. Indeed, given any $C^1$ function $Y = Y(t, n)$ such that $X - Y$ has a local maximum at $(t_0, n_0)$. Without loss of generality, we assume $X(t_0, n_0) - Y(t_0, n_0) = 0$. We focus on the 2-dimensional plane $\Gamma_0$ by fixing $t = t_0$ (see Fig. 2).

Since $X - Y$ attains a local maximum at $(t_0, n_0)$, by (2.18) there must hold

$$\frac{\partial}{\partial n} Y(t_0, n_0) < 0$$

**Fig. 2** Graphs of $X(t_0, \cdot)$ and $Y(t_0, \cdot)$
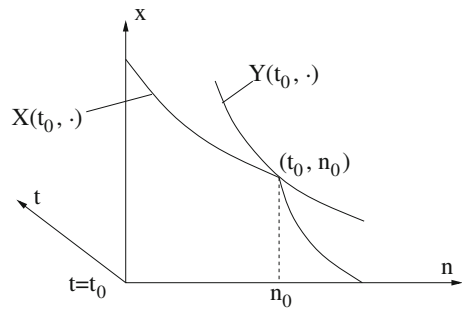


By $C^1$ continuity, there exists a neighborhood $\Omega_1$ of $(t_0, n_0)$ such that

$$\frac{\partial}{\partial n} Y(t, n) < 0 \qquad \forall (t, n) \in \Omega_1$$

Then, we may define $C^1$ function $M(t, x)$ such that $n = M(t_0, \cdot)$ is the inverse of $x = Y(t_0, \cdot)$ in $\Omega_1 \cap \Gamma_0$. In addition, $N - M$ attains a local maximum at $(t_0, X(t_0, n_0))$. We use the fact that $N(t, x)$ is a viscosity solution and apply (2.14) to get

$$M_t(t, x) \leq f(-M_x(t, x)) \tag{2.19}$$

Differentiating identity $Y(t, M(t, x)) = x$ w.r.t. $t$, and using (2.19), we deduce

$$0 = Y_t + Y_n M_t \geq Y_t + Y_n f(-M_x) = Y_t + Y_n f\left(-\frac{1}{Y_n}\right) = Y_t - \psi(Y_n) \tag{2.20}$$

Here we use the fact that $M(t, \cdot)$, $Y(t, \cdot)$ are both $C^1$ and inverse of each other,

$$\frac{d}{dn}\{n = M(t, Y(t, n)\} \implies 1 = M_x \cdot Y_n$$

Since $Y$ is arbitrary, (2.20) implies that $X(t, n)$ is a subsolution. The case for supersolution is completely similar.                                                          $\square$

*Remark 2.5* Similar proof can be used to show the reverse: given a viscosity solution $X(\cdot, \cdot)$ to (2.17), then $N(t, \cdot)$ obtained via inverting $X(t, \cdot)$ provides a viscosity solution to (2.16).

   Theorem 2.4 establishes equivalence of Hamilton Jacobi equations in the two coordinate systems, in the sense of viscosity solution. We proceed in the next section to explore its applications to traffic data fusion and state estimation. This requires a solution method that is capable of incorporating mobile and fixed data with large quantity and high dimensions. The class of viscosity solutions, despite their mathematical rigor, suffer from existence problems in the presence of multiple value conditions (initial, boundary and internal boundary conditions). Thus, we turn to a more general solution class known as the viability solutions developed in Aubin (2009), Aubin et al. (2008), and Claudel and Bayen (2010a).

## 3 Numerical Algorithm and Value Conditions

In this section, we focus on numerical solution to the Hamilton-Jacobi equation

$$\partial_t X(t, n) - \psi\left(-\partial_n X(t, n)\right) = 0 \qquad (3.21)$$

given initial/intermediate condition, boundary condition and internal boundary conditions, to be precisely defined below. One question arises as how to define a proper solution to the problem when the viscosity solution satisfying (3.21) do not necessarily satisfy the numerous value conditions. The viability theory (Aubin 2009; Aubin et al. 2008) provides appropriate tools to answer this question, by constructing a semi-analytical solution to the problem using the Lax-Hopf formula (Claudel and Bayen 2010a, b). The resulting solution is the lower-semicontinuous Barron Jensen/Frankowska solution (Barron and Jensen 1990; Frankowska 1993), which will be discussed in Section 3.1. For practical reasons, we only discuss the application of viability theory to Hamilton-Jacobi Eq. (3.21), while referring the readers to Aubin (2009) for more background on viability theory. Section 3.2 defines the value conditions and interprets their meanings in relation to the two coordinate systems.

### 3.1 Viability Episolution to the Hamilton-Jacobi Equation (3.21)

This section presents the viability episolution (Claudel and Bayen 2010a) and its solution method known as the generalized Lax-Hopf formula. We first define the domain of Eq. (3.21):

$$(t, n) \in [0, T] \times [N_1, N_2]$$

for some $T > 0$; $N_1, N_2$ represent upstream boundary and downstream boundary of the Lagrangian domain. In the following definition, we define the value condition for (3.21), which is a generalization of initial condition and boundary condition, and conditions prescribed inside the domain.

**Definition 3.1** A value condition $\mathcal{C}(\cdot, \cdot)$ is a lower-semicontinuous function from a subset $\Omega$ of $[0, T] \times [N_1, N_2]$ to $\mathbb{R}$

The value condition may be extended to the whole domain by assigning $\mathcal{C}(t, n) = +\infty$ whenever $(t, n) \notin \Omega$. This convention enables us to compare and manipulate value conditions with different domains. We introduce the concave transformation of Hamiltonian $\psi(\cdot)$:

$$\psi^*(u) \doteq \sup_{s \in [1/\rho_{\max}, +\infty)} \{\psi(s) - u\,s\}$$

The following generalized Lax-Hopf formula provides semi-analytical viability episolution (Aubin et al. 2008; Claudel and Bayen 2010a).

**Theorem 3.2** *The viability episolution to* (3.21) *associated with value condition* $\mathcal{C}(\cdot, \cdot)$ *is characterized by the Lax-Hopf formula*

$$X_{\mathcal{C}}(t, n) = \inf_{(u, T) \in Dom(\psi^*) \times \mathbb{R}_+} \left( \mathcal{C}(t - T, x + T u) + T \psi^*(u) \right) \qquad (3.22)$$

*Proof* See Claudel and Bayen (2010a)                                                □

For a solution of the Hamilton-Jacobi equation, we indicate its dependence on the value condition $\mathcal{C}$ by a subscript. Equation (3.22) implies an important inf-morphism property (Aubin et al. 2008; Claudel and Bayen 2010a)

**Proposition 3.3** *(inf-morphism property) Let* $\mathcal{C}(\cdot, \cdot)$ *be the minimum of finitely many value conditions,*

$$\mathcal{C}(t, n) \doteq \min_{i=1,\dots,m} \mathcal{C}_i(t, n) \qquad \forall \ (t, n) \in [0, T] \times [N_1, N_2]$$

*Then*

$$X_{\mathcal{C}}(t, n) = \min_{i=1,\dots,m} X_{\mathcal{C}_i}(t, n) \qquad (3.23)$$

This property allows the PDE to incorporate an arbitrary number of value conditions; it also decomposes a complex problem involving multiple value conditions into smaller subproblems, each with a single value condition.

### 3.2 Value Conditions for Continuous Solutions

The value conditions described in the previous section are mathematical representations of real traffic measurements; according to the source of data, they can be categorized as Eulerian sensing and Lagrangian sensing. The former refers to quantities measured with fixed location such as loop detector and video camera, the latter are obtained from on-board devices with continuous positioning capabilities. It is demonstrated in Claudel and Bayen (2010a, b) that the Eulerian based Hamilton-Jacobi equation is capable of fusing both Eulerian and Lagrangian data. This section shows that the same holds for Lagrangian-based equation.

We consider the continuous version of the value conditions associated with the Hamilton-Jacobi equations.

$$\partial_t M(t, x) - f \left( -\partial_x M(t, x) \right) = 0 \qquad \text{(Eulerian based)} \qquad (3.24)$$

$$\partial_t X(t, n) - \psi \left( -\partial_n X(t, n) \right) = 0 \qquad \text{(Lagrangian based)} \qquad (3.25)$$

To illustrate the connection between value conditions in the two coordinate systems, we make a few assumptions on the value condition $\mathcal{C}$.

**(A1)**   The domain of $\mathcal{C}$ is a continuous curve parametrized by $\tau \in [\tau_{\min}, \tau_{\max}]$:

$$\text{Dom}(\mathcal{C}) \subset [0, T] \times [N_1, N_2] \qquad (\text{respectively } [0, T] \times [X_1, X_2])$$

$$\text{Dom}(\mathcal{C}) = (t(\tau), n(\tau)) \qquad (\text{respectively } (t(\tau), x(\tau)))$$

$$\tau \in [\tau_{\min}, \tau_{\max}]$$

**(A2)**   $\mathcal{C}(t(\cdot),\, n(\cdot))$ is a continuous function on $[\tau_{\min},\, \tau_{\max}]$.

Given a continuous value condition $\mathcal{C}$ for (3.24), whose domain is a subset of the $x - t$ plane, question arises as how to fuse this into the Lagrangian based equation. Intuitively, one needs to switch the domain and range of $\mathcal{C}$ before applying it to (3.25). The next proposition shows that this is indeed the case.

**Proposition 3.4** *(Sufficient condition for equivalence of value conditions)*
*Let $\mathcal{C}^E(t(\tau),\, x(\tau))$ and $\mathcal{C}^L(t(\tau),\, n(\tau))$, $\tau \in [\tau_{\min},\, \tau_{\max}]$ be two value conditions for (3.24) and (3.25), respectively. Then the solutions to (3.24) and (3.25) satisfying each value condition are equivalent if*

$$n(\tau) \,=\, \mathcal{C}^E(t(\tau),\, x(\tau)), \qquad x(\tau) \,=\, \mathcal{C}^L(t(\tau),\, n(\tau))$$

*Proof* Let $N_{\mathcal{C}^E}(t,\, x)$ be the solution to (3.24) satisfying condition $\mathcal{C}^E$, let $X_{\mathcal{C}^L}(t,\, n)$ be the solution to (3.25) satisfying condition $\mathcal{C}^L$. For each $t$, since $N_{\mathcal{C}^E}(t,\, \cdot)$ is strictly increasing, we denote its inverse by $N_{\mathcal{C}^E}^{-1}(t,\, \cdot)$. Then by Theorem 2.4, $N_{\mathcal{C}^E}^{-1}(\cdot,\, \cdot)$ is a valid solution to the HJ Eq. (3.25).

On the other hand, for every $\tau \in [\tau_{\min},\, \tau_{\max}]$,

$$N_{\mathcal{C}^E}^{-1}(t(\tau), n(\tau)) = N_{\mathcal{C}^E}^{-1}\Big(t(\tau), \mathcal{C}^E(t(\tau), x(\tau))\Big) = N_{\mathcal{C}^E}^{-1}\Big(t(\tau),\, N_{\mathcal{C}^E}(t(\tau), x(\tau))\Big) = x(\tau)$$

$$(3.26)$$

Equation (3.26) implies that $N_{\mathcal{C}^E}^{-1}(\cdot,\, \cdot)$ satisfies the value condition $\mathcal{C}^L(t(\tau),\, n(\tau))$ and thus is the unique solution to (3.25) associated with value condition $\mathcal{C}^L$. We conclude $N_{\mathcal{C}^E}^{-1}(t,\, n) = X_{\mathcal{C}^L}(t,\, n)$.                                            $\square$

*Example 1* Consider an Eulerian sensor (such as a loop detector) that counts the passing vehicles at location $x_0$ during time interval $[t_1,\, t_2]$. Suppose the domain and measurement of the value condition $\mathcal{C}^E$ provided by this sensor are shown in Figs. 3 and 4, respectively. Let $N_{\mathcal{C}^E}(t,\, x)$ be the viability solution. We define value condition $\mathcal{C}^L$ with domain depicted in Fig. 4 and value in Fig. 3; applying it to the Lagrangian based equation yields equivalent solution to $N_{\mathcal{C}^E}$.

This section addresses two important aspects of the Lagrangian based PDE: numerical method and value conditions. It is seen from Proposition 3.4 that value conditions in either coordinate system can be easily integrated into the equation of the other. In the next section, we articulate the piecewise affine value conditions and compute the analytical solution of Eq. (3.25) with these conditions.

## 4 Solution with Piecewise Affine (PWA) Value Conditions

In this section we apply the Lax-Hopf formula (3.22) to obtain closed form solution. We assume *piecewise affine* (PWA) initial, boundary and internal boundary conditions for the Hamilton-Jacobi Eq. (2.11), which is equivalent to requiring piecewise

**Fig. 3** Domain of $\mathcal{C}^E$
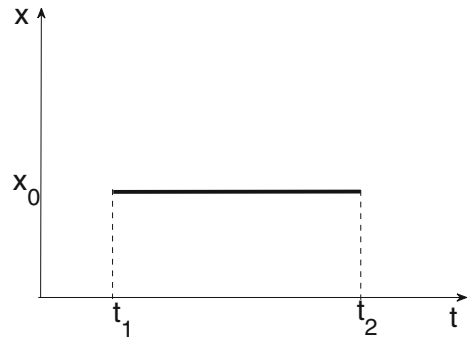


constant spacing and velocity values. This assumption enables us to construct closed-form solutions. Due to the fact that any function with certain regularity (e.g. piecewise continuous) can be well approximated using linear spline functions, the PWA assumption is not restrictive in application.

It has been observed in Leclercq et al. (2007) and Yuan et al. (2011) that the Lagrangian based conservation law (2.12) has some numerical advantages over the Eulerian based equation since the flux function $\psi(\cdot)$ is monotonic, and as a result the Godunov finite difference method reduces to a simple upwind scheme. In this section we have similar observations by comparing the viability solutions in both coordinates: we are able to unify the upstream/downstream and internal boundary conditions into one type of condition and solve for it using one single formula.

Section 4.1 explicitly defines piecewise affine initial/intermediate, upstream/ downstream and internal boundary conditions; in Section 4.2, we present explicit formula for viability episolution with a simple flux function.

### 4.1 Piecewise Affine Value Conditions

We start with articulating the simple piecewise affine value conditions, including initial (intermediate), upstream, downstream and internal conditions. These are building blocks of more complicated PWA value conditions.

**Fig. 4** Measurement of $\mathcal{C}^E$
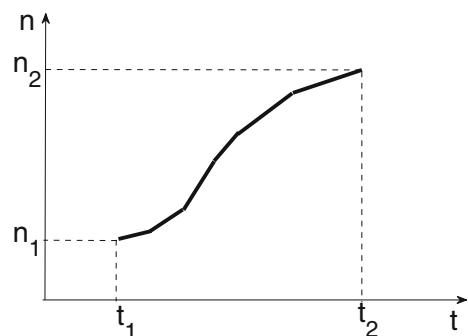
**Definition 4.1 (PWA initial/intermediate condition).** Set $t = t_0 \geq 0$, given real numbers $s_i \geq 0$, $n_i$, $i \in \{1, \ldots, m_{ini}\}$, the $j^{th}$ affine component of initial/intermediate condition is

$$\mathcal{C}_{ini}(t_0, n) = -s_j n + d_j, \qquad n \in [n_j, n_{j+1}] \tag{4.27}$$

To ensure continuity, we require

$$d_j = s_j n_j - \sum_{l=1}^{j-1}(n_{l+1} - n_l), \qquad j = 2, \ldots, m_{ini}$$

**Definition 4.2 (PWA upstream boundary condition).** Fix $n = N_1$, given real numbers $v^i \geq 0$, $t^i$, $i \in \{1, \ldots, m_{up}\}$, the $j^{th}$ affine component of upstream boundary condition is defined as

$$\mathcal{C}_{up}^j(t, N_1) = v^j t + b^j, \qquad t \in [t^j, t^{j+1}] \tag{4.28}$$

To ensure continuity of upstream boundary condition, we set

$$b^j = -v^j t^j + \sum_{l=1}^{j-1}(t^{l+1} - t^l)v^l, \qquad j = 2, \ldots, m_{up}$$

**Definition 4.3 (PWA downstream boundary condition).** Fix $n = N_2$, given real numbers $v_i \geq 0$, $t_i$, $i \in \{1, \ldots, m_{down}\}$, the $j^{th}$ affine component of downstream boundary condition is defined as

$$\mathcal{C}_{down}^j(t, n) = v_j t + b_j, \qquad (t, n) \in [t_j, t_{j+1}] \times \{N_2\} \tag{4.29}$$

where

$$b_j = -v_j t_j + \sum_{l=1}^{j-1}(t_{l+1} - t_l)v_l, \qquad j = 1, \ldots, m_{down}$$

**Definition 4.4 (Affine internal boundary condition).** Given real numbers $\alpha$, $\beta$, $t_{min}, t_{max}, n_{min}, n_{max}$, and $r \geq 0$, the affine internal boundary condition is defined as

$$\mathcal{C}_{int}(t, n) = \beta + \alpha(t - t_{min}) \qquad t \in [t_{min}, t_{max}], \quad n = n_{min} + r(t - t_{min}) \tag{4.30}$$

Recall that the domain of our consideration is $[0, T] \times [N_1, N_2]$, thus the upstream/downstream boundary conditions refer to (part of) the trajectories of the first and last car within our scope.

## 4.2 Explicit Formulae for Viability Episolutions

In the presence of piecewise affine (PWA) data, the solution of Lagrangian Eq. (3.25) with any continuous and concave Hamiltonian can be computed explicitly using Lax-Hopf formula (3.22), as in Claudel and Bayen (2010a, b). We are going to, in

this article, derive formulae with a simple Hamiltonian $\psi(s)$ corresponding to the triangular fundamental diagram:

$$f(\rho) = \begin{cases} v_{\max}\,\rho & \rho \in [0,\,\rho^*] \\ v_b(\rho_{\max} - \rho) & \rho \in (\rho^*,\,\rho_{\max}] \end{cases}$$

where $v_{\max} > 0$ and $v_b > 0$ denote the forward and backward kinematic wave speeds, respectively; $v_{\max}$ also represents the maximum vehicle speed. $\rho^*$ and $\rho_{\max}$ denote, respectively, the critical and maximum densities. Following these notations, we define $s_{\min} \doteq 1/\rho_{\max}$, $s^* \doteq 1/\rho^*$, and

$$\psi(s) = \begin{cases} k(s - s_{\min}) & s \in [s_{\min},\, s^*] \\ v_{\max} & s \in (s^*,\, +\infty) \end{cases} \tag{4.31}$$

where $k \doteq v_b \cdot \rho_{\max}$, which is immediately derived from the relationship between $\psi(\cdot)$ and the triangular fundamental diagram $f(\cdot)$, as shown in Fig. 1. Moreover, the concave conjugate of $\psi$ reduces to

$$\psi^*(u) = s^*(k - u) - ks_{\min} = s^*(k - u) - v_b \qquad u \in [0,\, k] \tag{4.32}$$

**Proposition 4.5** *With the affine value conditions defined in (4.27)–(4.30), and assuming a Hamiltonian (4.31), the solutions to the Lagrangian Hamilton-Jacobi Eq. (3.25) can be explicitly expressed as*

1. *PWA Initial/intermediate value problem*
   if $s_j \le s^*$,

$$X_{ini}^j(t,\,n) = \begin{cases} -s_j n + d_j + (t - t_0)(ks_j - v_b), \\ n_j + k(t - t_0) \le n \le n_{j+1} + k(t - t_0); \\ \\ -s_j n_j + d_j + (t - t_0)v_{\max} - s^*(n - n_j), \\ 0 \le n - n_j \le k(t - t_0). \end{cases} \tag{4.33}$$

   if $s_j > s^*$,

$$X_{ini}^j(t,\,n) = \begin{cases} -s_j n_{j+1} + d_j + (t - t_0)v_{\max} - s^*(n - n_{j+1}), \\ 0 \le n - n_{j+1} \le k(t - t_0); \\ \\ -s_j n + d_j + v_{\max}(t - t_0), \\ n_j \le n \le n_{j+1}. \end{cases} \tag{4.34}$$

2. *Upstream boundary value problem*

$$X_{up}^j(t,\,n) = \begin{cases} v^j t^{j+1} + b^j + v_{\max}(t - t^{j+1}) - s^*(n - N_1), \\ 0 \le n - N_1 \le k(t - t^{j+1}); \\ \\ v^j t + b^j - (n - N_1)\dfrac{v^j + v_b}{k}, \\ \max\{0,\, k(t - t^{j+1})\} \le n - N_1 \le k(t - t^j). \end{cases} \tag{4.35}$$

3. *Downstream boundary value problem*

$$X_{down}^{j}(t, x) = v_j\, t_{j+1} + b_j + (t - t_{j+1})\, v_{max}, \quad (t, x) \in [t_{j+1}, +\infty) \times \{N_2\} \tag{4.36}$$

4. *Internal boundary value problem*

$$X_{int}(t, n) = \begin{cases} \beta + \alpha(t - t_{min}) + (\alpha + v_b)\dfrac{n - n_{min} - r(t - t_{min})}{r - k} \\ r\,(t - t_{min}) \le n - n_{min} \le k(t - t_{min}) \ and \\ k(t - t_{max}) < n - n_{max}; \\[2mm] \beta + \dfrac{n - n_{min}}{r}\alpha + v_{max}\left(t - t_{min} - \dfrac{n - n_{min}}{r}\right) \\ 0 \le n - n_{min} < r(t - t_{min}) \quad and \quad n \le n_{max}; \\[2mm] \beta + \alpha\,(t_{max} - t_{min}) + (t - t_{max})v_{max} - s^*\,(n - n_{max}), \\ 0 \le n - n_{max} \le k(t - t_{max}). \end{cases} \tag{4.37}$$

*Remark 4.6* (4.37) is well defined even for cases $k = r$ and $r = 0$.

*Proof* Apply the Lax formula to the piecewise conditions (4.27)–(4.30) and $\psi^*$, verifying (4.33)–(4.37) are straightforward.                                □

It turns out that the formulae for upstream, downstream and internal boundary conditions (4.35)–(4.37) can be unified into one. In other words, the upstream and downstream conditions can be treated as spacial cases of internal boundary conditions. Indeed, since the wave speed in the Lagrangian equation is always non-negative, the value conditions only influence the region with larger $n$; see Fig. 5 for an example. This coincides with the observation that traffic conditions experienced by some vehicles cannot affect vehicles in front of them (with smaller $n$).

**Proposition 4.7** *Each $j$-th component of* (4.28) *and* (4.29) *can be rewritten as* (4.30) *with $r = 0$, $n_{max} = N_1$ and $r = 0$, $n_{min} = N_2$, respectively. Furthermore, with this specification,* (4.35) *and* (4.36) *coincide with* (4.37).

*Proof* To verify the equivalence between (4.35), (4.36) and (4.37), notice that the second part of (4.37) is infeasible for $s = 0$, and the rest is directly checked.     □

We have so far expressed the solution for each type of condition in Proposition 4.5. To compute the solution taking into account contributions of all value conditions, we invoke the inf-morphism property in Proposition 3.3 and take the minimum over all solutions (4.33), (4.34) and (4.37).

The numerical performance of the aforementioned algorithm is enhanced in two ways. First, each solution (4.33), (4.34) and (4.37) is expressed explicitly and free of spatial discretization; second, the algorithm is highly parallelizable: the full problem
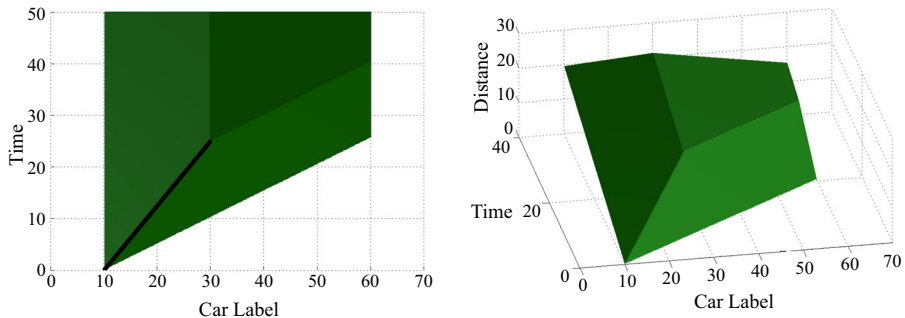
**Fig. 5** Left: range of influence of an internal boundary condition (black line). Regions represented in (4.37) can be seen clearly. Value of this condition cannot propagate backward to the region $n < 10$. Right: 3d demonstration of the solution to the internal boundary value problem

can be decomposed into sub-problems involving simple value conditions, and each sub-task is independent of each other.

In summary, we have established the LWR model in transformed coordinates and justified the new Hamilton-Jacobi equation; both Eulerian sensing and Lagrangian sensing have been integrated into the Lagrangian based equation, whose solution is solved in closed form in conjunction with various value conditions. As an application of the model and solution method, we will conduct a numerical study of highway traffic estimation in Section 5.

# 5 Numerical Study

## 5.1 The Mobile Century Field Experiment

On February 8, 2008, an experiment in traffic monitoring, nicknamed the *Mobile Century*, was launched between 9:30 am to 6:30 pm on freeway I-880 near Union City in the San Francisco Bay Area, California. This experiment involved 100 vehicles carrying GPS-enabled Nokia N95 phones, which repeatedly drove loops of 6-10 miles in length continuously for 8 hours.

Carried by each probing vehicle, the smart phone was storing its position and velocity every 3-4 seconds, which allowed the trajectory of the equipped vehicle to be computed. In addition to the cell phone GPS data, inductive loop detector data obtained through the *Freeway Performance Measurement System* (PeMs) database are available. The readers are referred to Herrera et al. (2009) for more details of experimental design and data description.

## 5.2 Numerical Implementation

The freeway segment of interest is a 3.45 mile stretch of I-880 North Bound, between PeMS station 400536 (23.36 postmile), to postmile 26.82. There are two sources of data, the cumulative vehicle count, obtained via loop detector station 400536, which

counted passing vehicles every 30 s, and on-board smart phones recording vehicle velocity and trajectory every 3-4 s. The time period of our measurement is 1 hour from 11:30 am to 12:30 pm, which involves approximately 5000 vehicles. We take into account 97 mobile data samples, as well as vehicle count obtained from Station 400536 in order to label our probing vehicles.

We consider the freeway segment as a homogeneous road, and seek a unique fundamental diagram $f(\cdot)$ for the density-flow relation or $\psi(\cdot)$ for the spacing-velocity relation. We prefer to utilize data collected in the experiment for the best functional fitting. Unfortunately, we do not have access to either the maximal density $\rho_{max}$, or an appropriate way to measure it directly. Instead, we take advantage of the relation

$$f(\rho) = \rho \, v(\rho) \tag{5.38}$$

and collect flow as well as velocity data. More precisely, for appropriate time instance $t_0$, we estimate the flow through Station 400536 using a 30 s vehicle count, and record the velocity of the probing vehicles passing the same location at $t_0$. Then, density is estimated as the quotient of flow and velocity. Scatter plots of 324 samples are shown in Figs. 6 and 7.

For a triangular density-flow relationship depicted in Fig. 6, the parameters are chosen to be

$$f(\rho) = \begin{cases} v_{max} \, \rho & \rho \in [0, \, \rho^*] \\ v_b \, (\rho_{max} - \rho) & \rho \in (\rho^*, \, \rho_{max}] \end{cases} \tag{5.39}$$

$$v_{max} = 31.5 \text{ m/s}, \quad v_b = 3.90 \text{ m/s}, \quad \rho^* = 0.055 \text{ veh/m}, \quad \rho_{max} = 0.50 \text{ veh/m}. \tag{5.40}$$

where $v_{max}$, $v_b$, $\rho^*$, $\rho_{max}$ are respectively, free flow speed, backward-propagating kinematic wave speed, critical density and maximal (jam) density. For the corresponding spacing-velocity relationship, the parameters are chosen to be

$$\psi(s) = \begin{cases} k(s - s_{min}) & s \in [s_{min}, \, s^*] \\ v_{max} & s \in (s^*, \, +\infty) \end{cases} \tag{5.41}$$

$$k = 1.95 \text{ veh/s}, \quad s_{min} = 2.00 \text{ m/veh}, \quad s^* = 18.15 \text{ m/veh}, \quad v_{max} = 31.5 \text{ m/s}. \tag{5.42}$$

where $s_{min}$ and $s^*$ are minimum and critical spacings, respectively.

## 5.3 Numerical Results

As an application of the Hamilton-Jacobi equation in Lagrangian coordinates and viability episolution, we will reconstruct the traffic state between postmile 23.36 and 26.82, for a time period of one hour, using only Lagrangian sensing. Figure 8 shows 97 mobile data we utilize for this numerical experiment. For the viability solution to the Hamilton-Jacobi Eq. (3.21), we use internal boundary conditions based on trajectories of 44 probing vehicles, which account for 0.88% of the total monitored traffic volume. Notice that the on-board sensors recorded vehicle position every 3-4 seconds, this implies approximately 100-300 sample points per vehicle, among which we only utilize 10 sample points, this is for numerical simplicity and also shows robustness of the algorithm.
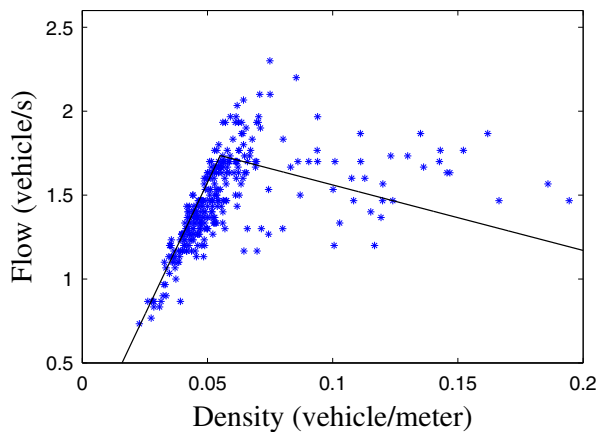
**Fig. 6** Density-flow relationship

One task of Lagrangian traffic estimation is the construction of vehicle trajectories. Given the solution $X(\cdot, \cdot)$, for a car labeled $n_0$, the estimated trajectory is simply $X(\cdot, n_0)$. Two examples, including both estimated trajectory and measurement obtained from mobile sensors, are shown in Figs. 9 and 10.

A partial solution based on 8 internal boundary conditions obtained via mobile sensors are shown in Fig. 11. It should be noted that the viability solution only satisfies inequality constraints, i.e.

$$X_{\mathcal{C}}(t, n) \leq \mathcal{C}(t, n), \qquad (t, n) \in \mathrm{Dom}(\mathcal{C})$$

In case of strict inequality, the value conditions and the model are said to be incompatible. The incompatibility is due to either measurement error or modeling error,
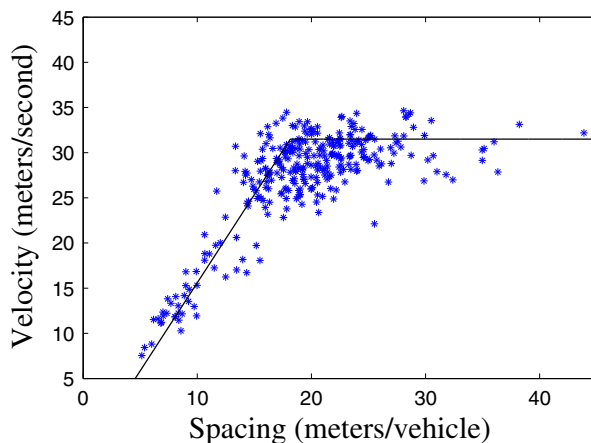


**Fig. 7** Spacing-velocity relationship
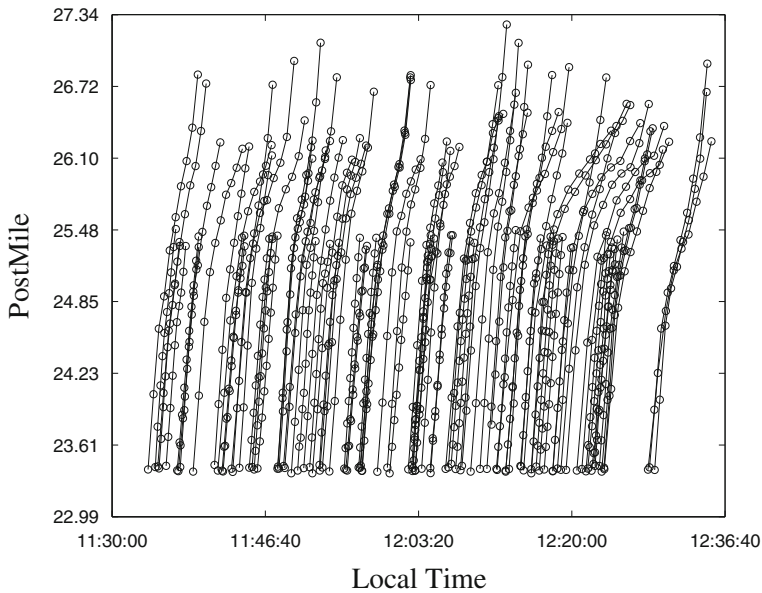
**Fig. 8** Plots of probing vehicle trajectories used to cover the freeway segment during the study period

this gives rise to the issues of data assimilation and reconciliation, in which modeling parameters, or sensing data, are tuned to best fit each other. The readers are referred to Claudel and Bayen (2011) for full details.
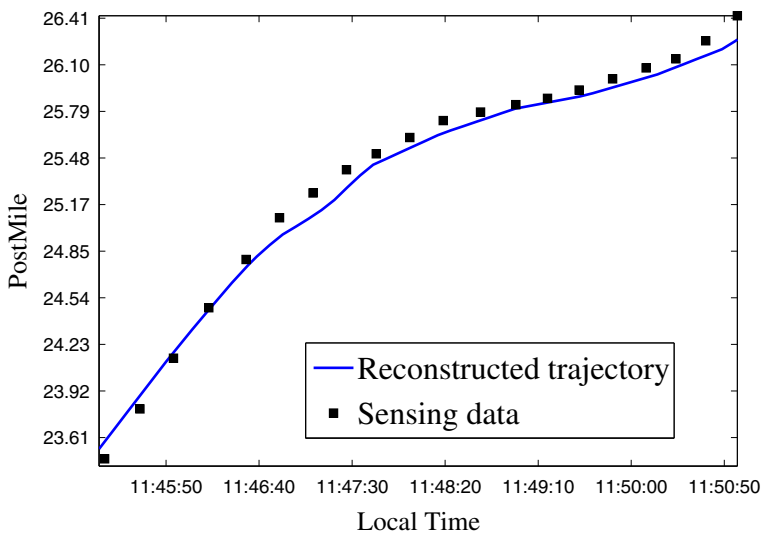


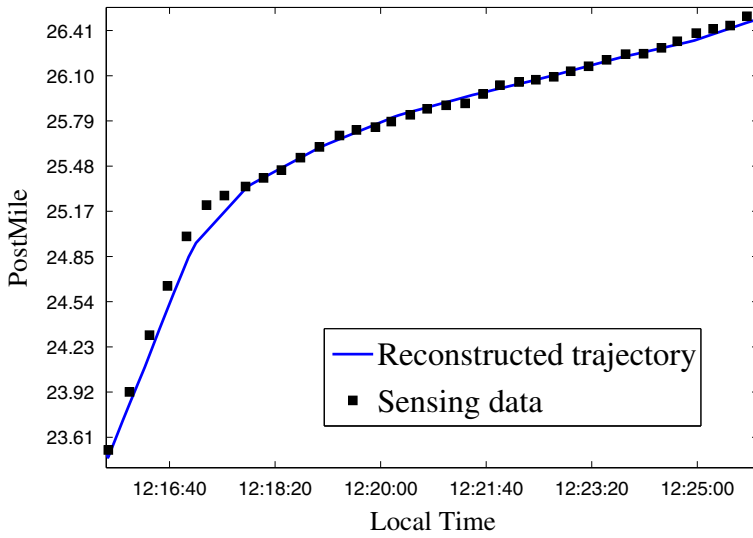**Fig. 9** Estimated and true trajectory of vehicle #8685
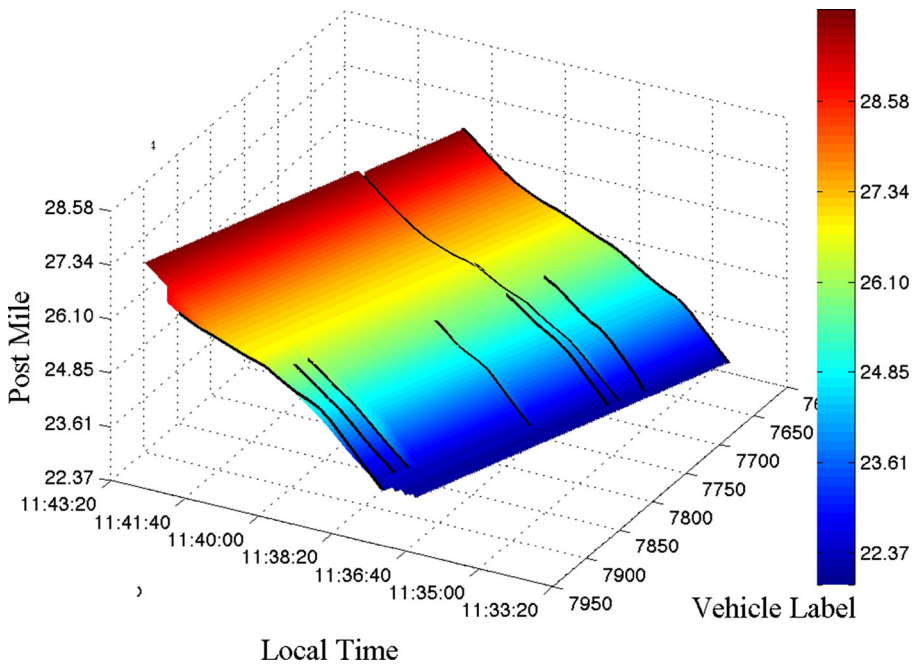
**Fig. 10** Estimated and true trajectory of vehicle #11266



**Fig. 11** Solution of Hamilton-Jacobi Eq. (3.21) with 8 internal boundary conditions, solid lines are vehicle trajectories recorded by mobile sensors
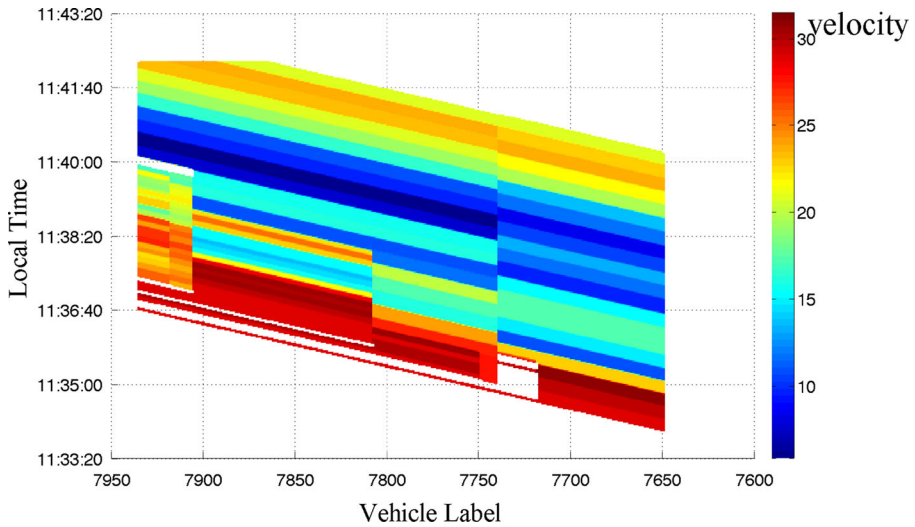
**Fig. 12** Vehicle velocity (m/s) estimation based on (5.43)

Based on the solution $X(t, n)$, we can further estimate vehicle-based velocity, via

$$\partial_t X(t, n) = \psi(s(t, n)) = v(t, n) \qquad (5.43)$$

Figure 12 shows the velocity field involving vehicle labels ranging from $7650 - 7950$. From this picture, we observe time-varying traffic conditions from free flow to congestion then back to uncongested traffic. This phenomenon is also reflected in Fig. 8, where all vehicles seemed to experience a slow down whithin postmile $25.5 - 26.3$.
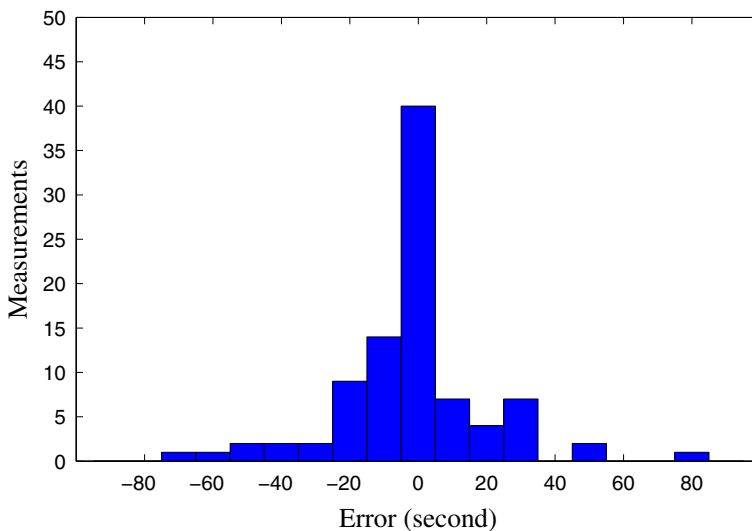


**Fig. 13** Summary of errors for travel time estimation

In order to examine the accuracy of travel time estimation, we compare the actual travel times of 97 probing vehicles with the estimated travel times obtained from the reconstructed trajectories. The results are summarized in Fig. 13. Note that, given the travel times through the study area ranging from 5-10 min, the errors shown in this figure are considered minor, which demonstrates the effectiveness of the proposed model in travel time estimation.

## 6 Conclusion

This article presents the Lagrangian coordinate system in the hydrodynamic traffic model, and studies the Hamilton-Jacobi equation describing traffic quantities associated with moving vehicles. A numerical algorithm capable of fusing high dimensional mobile data is applied to highway traffic flows and yields promising results in terms of traffic reconstruction and travel time estimation.

Compared to Eulerian based LWR model, the Lagrangian approach models traffic flows in a moving reference frame, and the corresponding PDE provides knowledge of vehicle based quantities such as trajectory and speed. We have also demonstrated a few numerical advantages in the Lagrangian-based Hamilton-Jacobi equation due to monotonic hamiltonian.

A well-developed theory on Lagrangian-based traffic models will lead to more mature modeling and computational methodologies as well as more advanced applications to the cyber-physical traffic systems such as car-to-car networking and mobile internet. For future work, more refined models need to be developed, taking into account the modeling uncertainty such as vehicle inhomogeneity and car overtaking. Extension to network will be of great interest, although this is mathematically more challenging.

## References

Aubin JP (2009) Viability theory. Springer Science & Business Media, Berlin

Aubin JP, Bayen AM, Saint-Pierre P (2008) Dirichlet problems for some Hamilton-Jacobi equations with inequality constraints. SIAM J Control Optim 47(5):2348–2380

Barron EN, Jensen R (1990) Semicontinuous viscosity solutions for Hamilton-Jacobi equations with convex Hamiltonians. Comm Partial Differential Equations 15:1713–1742

Bressan A (2000) Hyperbolic systems of conservation laws. The One Dimensional Cauchy Problem. Oxford University Press, Oxford

Bressan A, Han K (2011) Optima and Equilibria for a model of traffic flow. SIAM J Math Anal 43(5):2384–2417

Bressan A, Han K (2012) Nash equilibria for a model of traffic flow with several groups of drivers. ESAIM: Control Optimization and Calculus of Variations 18(4):969–986

Claudel CG, Bayen AM (2011) Convex formulations of data assimilation problems for a class of Hamilton-Jacobi equations. SIAM J Control Optim 49(2):383–402

Claudel CG, Bayen AM (2010a) Lax-Hopf Based incorporation of internal boundary conditions into Hamilton-Jacobi equation. Part I: Theory. IEEE Trans Autom Control 55(5):1142–1157

Claudel CG, Bayen AM (2010b) Lax-hopf based incorporation of internal boundary conditions into Hamilton-Jacobi equation. Part II: computational methods. IEEE Trans Autom Control 55(5):1158–1174

Courant R, Friedrichs KO (1999) Supersonic flows and shock wave, vol 21. Springer Science & Business Media

Daganzo CF (2005) A variational formulation of kinematic waves: basic theory and complex boundary conditions. Transp Res B 39(2):187–196

Daganzo CF (2006) On the variational theory of traffic flow: well-posedness, duality and applications. Networks and Heterogeneous Media 1(4):601–619

Evans LC (2010) Partial differential equations, 2nd edn. American Mathematical Society, Providence

Frankowska H (1993) Lower semicontinuous solutions of Hamilton-Jacobi-Bellman equations. SIAM J Control Optim 31(1):257–272

Garavello M, Han K, Piccoli B (2016) Models for vehicular traffic on networks. AIMS series on applied mathematics, Springfield

Godunov SK (1959) A difference scheme for numerical computation of discontinuous soulutions of equations of fluid dynamics. Mat Sb 47:271–290

Herrera JC, Work DB, Herring R, Ban XJ, Jacobson Q, Bayen AM (2009) Evaluation of traffic data obtained via GPS-enabled mobile phones: the mobile century field experiment. Transportation Research Part C: Emerging Technologies 18:568–583

Laval J, Leclercq L (2013) The Hamilton-Jacobi partial differential equation and the three representations of traffic flow. Transp Res B Methodol 52:17–30

Leclercq L, Laval J, Chevallier E (2007) The Lagrangian coordinate system and what it means for first order traffic flow models. In: Proceedings of the 17-th international symposium on transportation and traffic theory. London

Le Floch P (1988) Explicit formula for scalar non-linear conservation laws with boundary condition. Math Models Appl Sci 10:265–287

LeVeque RJ (1902) Numerical methods for conservation laws. Birkhäuser, Basel

Lighthill MJ, Whitham JB (1955) On kinematic waves II: a theory of traffic flow in long crowded roads. Proc R Soc A229:317–345

Mazare PE, Claudel CG, Bayen AM (2011) Analytical and grid-free solutions to the Lighthill-Whitham-Richards traffic flow model. Transport Res B 45(10):1727–1748

Moskowitz K (1965) Discussion of freeway level of service as influenced by volume and capacity characteristics. In: Drew DR, Keese CJ (eds) Highway research record, vol 99, pp 43–44

Newell GF (1993) A simplified theory of kinematic waves in highway traffic. Transp Res B 27B(4):281–303

Richards PI (1956) Shockwaves on the highway. Oper Res 4:42–51

Wagner D (1987) Equivalence of the Euler and Lagrangian equations of gas dynamics for weak solutions. J Diff Eq 68(1):118–136

Yuan Y, Van Lint JWC, Hoogendoorn SP, Vrancken JLM, Schreiter T (2011) Freeway traffic state estimation using extended kalman filter for first-order traffic model in lagrangian coordinates. In: 2011 international conference on networking, sensing and control. Netherlands